Supplementary information

Inside the Structure of a Nanocomposite Electrolyte Membrane: How Hybrid Particles Get Along with the Polymer Matrix

Manuel Maréchal,* Frédérick. Niepceron, Gérard Gebel, Hakima Mendil-Jakani and Hervé Galiano

S0-1. Synthesis of sodium poly(styrenesulfonate)-grafted silica particles[1]

Materials: Fumed silica (Sigma; particle size: 0.007 μm; surface area: 390 ± 40 m^2/g), referred to as A390, was dried under a nitrogen flow at 140 °C for 24 h before use. ((Chloromethyl)phenylethyl)trimethoxysilane (CPMS; ABCR), 2-2′-dipyridyl (Aldrich; 99+%), copper(I) chloride (CuCl; Sigma–Aldrich; 99.995%), 4-styrenesulfonic acid sodium salt (Aldrich) and sodium ethylenediaminetetra-acetate hydrate (EDTA; Aldrich; 98%) were used as received, as were toluene (Aldrich; anhydrous; 99.8%), methanol (VWR; rectapur), ethanol (VWR; rectapur; absolute), fuming sulfuric acid (H_2SO_4, Sigma–Aldrich) and *N*,*N*-dimethylformamide (DMF; Aldrich; anhydrous; 99.8%). Millipore® water was used in the preparation of aqueous solutions of the silica particles as well as for characterizing the composite membranes in terms of IEC, and proton-conductivity. A high molecular weight grade of a PVDF-HFP copolymer from Solvay (Solef® 21216) was selected for the preparation of the composite membranes.

Synthesis: In a first step, fumed silica particles were surface-modified with CPMS using a similar procedure to the one described by von Werne and Patten (see Fig. S0-1) in order to prepare initiator-grafted silica particles for surface-initiated atom transfer radical polymerization (ATRP) [2]. In a typical reaction, 15 g of fumed silica particles (equivalent to approx. 0.05 mol of surface silanols) were dispersed in 900 mL of toluene in a tri-necked 1 L round-bottomed flask under an argon flow. The dispersion was then brought to reflux at which time 25 mL of CPMS (0.1 mol) was added to the reaction mixture. The reaction was allowed to proceed for 4 h. After isolation, the surface-modified silica particles were thoroughly purified by two successive dispersion and centrifugation cycles in ethanol and acetone. The CPMS-grafted nanoparticles (~16 g) were then dried *in vacuo* at 60 °C overnight.

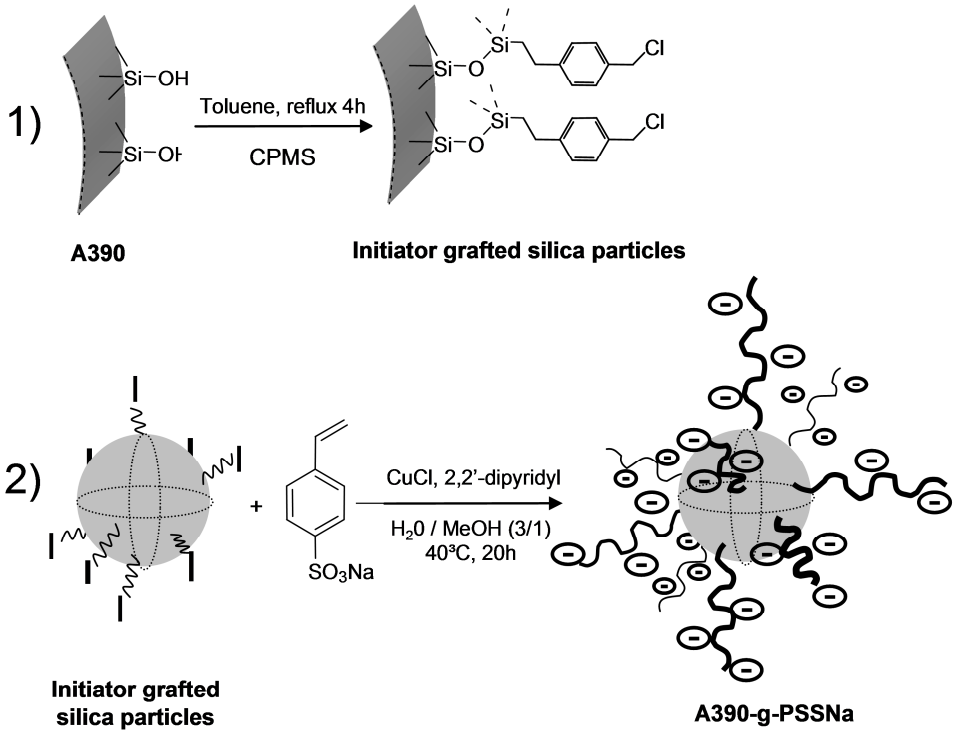

Figure S0-1. Synthetic route for the preparation of A390-g-PSSNa.

The initiator-grafted silica particles were used for the polymerization of sodium 4-styrenesulfonate. According to a typical protocol [3], surface-modified silica particles (15 g) were dispersed in 1250 mL of a 3:1 (v/v) water/methanol mixture under ultrasonic treatment. Sodium 4-styrenesulfonate (125 g, 0.6 mol) was added to the colloidal dispersion and stirred for 24 h. The reaction set-up was carefully degassed at low temperature under continuous stirring and left under a blanket of argon. CuCl (5 g, 0.05 mol) and 2,2′-dipyridine (15.8 g, 0.1 mol) were subsequently added under a flow of argon, the reaction mixture almost immediately turned dark brown, indicating the onset of the surface-initiated polymerization. The reaction was allowed to proceed for 20 h at 40 °C. Finally, the polymerization was terminated by exposure to air, causing the viscous dispersion to become blue due to the oxidation of Cu(I) to Cu(II). The supernatant was removed and the solid fraction was redispersed in deionized water under an ultrasonic treatment. The catalyst-contaminated sediment was purified with the aid of successive dispersion and centrifugation cycles in a diluted aqueous solution of EDTA (~6 g/L) in order to remove Cu(II) complexes giving rise to the characteristic blue color of the sediment. The dispersion–centrifugation cycle was repeated at least three times using fresh Millipore® water. Dispersions of the modified particles in water were then freeze-dried for 24 h in order to yield a nominally dry white powder (~30 g) of sodium poly(styrenesulfonate)-grafted silica particles, referred to as A390-g-PSSNa. The yield of the PSSNa grafting is only 15%.

S0-2. Characterization of particles

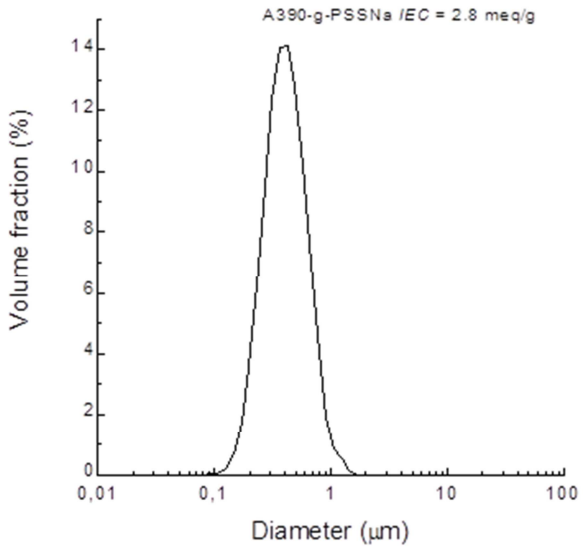

Figure S0-2a. Particle size distribution obtained by laser light scattering of PSSNa-grafted silica with an IEC=2.8 mequiv./g.

Figure S0-2a displays the particle size distribution of A390-g-PSSNa with an IEC of 2.8 mequiv./g was obtained by laser light scattering. A reasonable assumption of spherical particles was used in order to derive the particle diameters. It is worth noting that a thorough ultrasonic treatment was necessary prior to the measurements in order to suppress particle aggregates typically sized between 1 and 300 μm. The primary particle diameter was evaluated to 370 nm while a primary particle diameter of approx. 300 nm was obtained for particles with an IEC equal to 2.3 mequiv./g. Consequently, an increase in IEC could be directly coupled to an increase in the chain length of the PSSNa brushes, thus resulting in a growth of the shell size. Such a core–shell morphology was confirmed by the investigation of the morphological features of A390-g-PSSNa by CryoTEM (see Fig. S0-2b).

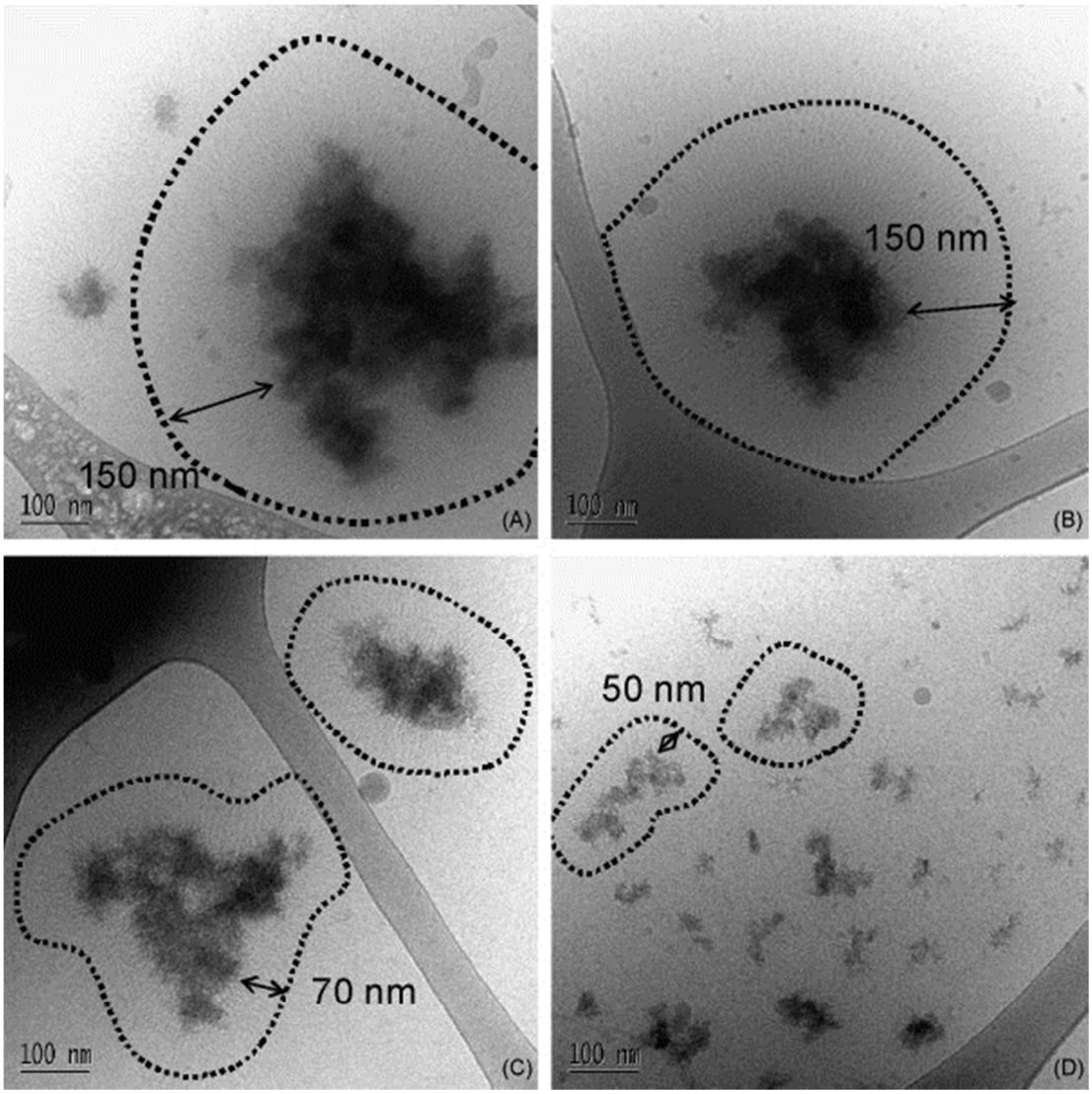

Figure S0-2b. Cryo-TEM micrographs of PSSNa-grafted silica with an IEC=2.8 mequiv./g.

The darker region in the figure represented the silica particles due to their high electronic density. The PSSNa chains can be observed in the form of low contrast brushes forming an organic shell around a silica core. The use of CryoTEM permitted an assessment of the size of the PSSNa shell that was comprised of elongated hydrophilic polymer segments. It could be observed that, regardless of the size of the particle, the PSSNa chains accounted for about half of the size of the silica core.

Table S1. Compositions of different composite membranes

Membrane filler content [wt.%]	Solution composition		
	Particles [wt.%]	PVDF-HFP [wt.%]	DMF [wt.%]
0	0	10	90
10	2	10	88
20	3	10	87
30	5	10	85
40	6	10	84
50	9	10	81
60	12	10	78
70	19	9	72

Table S2. Salts used for the preparation of statured solutions at 25°C, corresponding values of Relative Humidity, and λ (the number of water molecules per ionic site) for the membrane with a loading of 50 wt%.

salt	RH [%]	λ
LiCl	11	1.2
$KCOOCCH_3$	22	1.9
$MgCl_2$	32	2.3
$Mg(NO_3)_2$	52	3.2
NaCl	75	5.4
KCl	85	7.4
$BaCl_2$	90	10.9
$KClO_3$	98	32.3
water	100	106.8

Table S3. Structure parameters of the PVdF-HFP matrix (I_{cr} the crystallinity Index; $2\theta_{am}$ position of the amorphous halo; $2\theta_1$, $2\theta_2$ and $2\theta_3$, the positions of the crystalline reflections; w_1, w_2 and w_3, the corresponding half-widths (relative scale)).

Loading [wt.%]	I_{cr}	$2\theta_{am}$ [°]	$2\theta_1$ [°]	$2\theta_2$ [°]	$2\theta_3$ [°]	w_{am} [°]	w_1 [°]	w_2 [°]	w_3 [°]
0	0.270	21.70	20.82	23.31	31.31	7.44	1.67	0.80	3.01
10	0.183	22.35	20.80	23.26	31.31	7.34	1.66	0.75	2.97
20	0.177	22.34	20.77	23.72	31.26	7.30	1.32	0.80	2.80
30	0.165	22.31	20.69	23.62	31.35	8.26	1.31	1.30	3.00
40	0.143	22.60	20.97	23.66	31.39	8.55	1.35	1.25	3.13
50	0.137	22.89	20.75	23.57	31.65	9.89	1.30	1.24	3.11
60	0.137	23.41	20.93	23.65	31.89	9.49	1.31	1.20	3.02
70	0.127	23.72	20.93	23.80	31.63	9.49	1.31	1.20	3.00

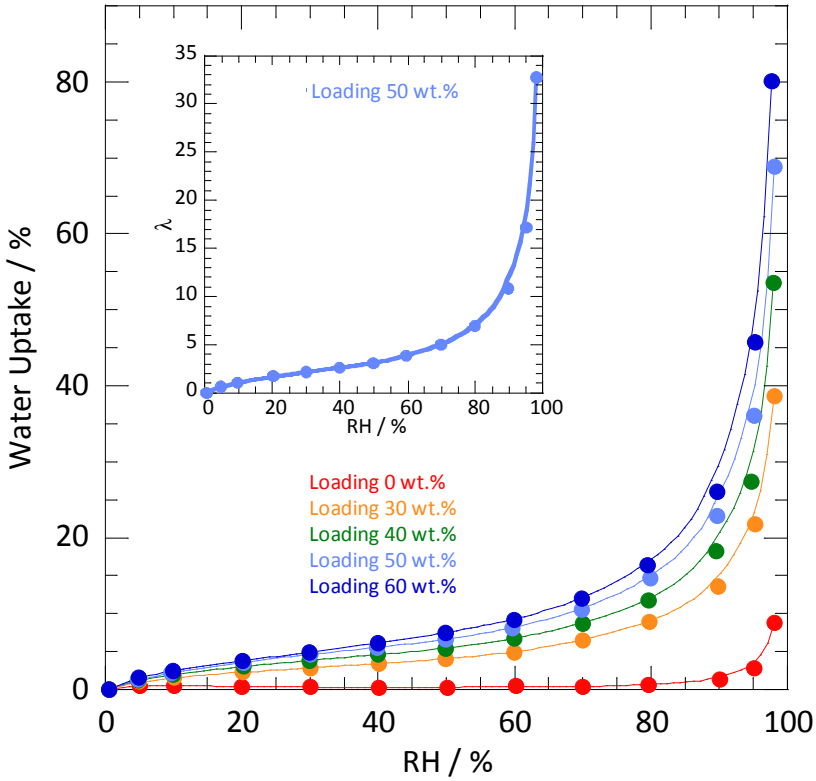

Figure. S1. Experimental sorption isotherms for different loadings. The experimental sorption isotherm λ=f(RH) is shown for 50 wt.% of loading in the inset.

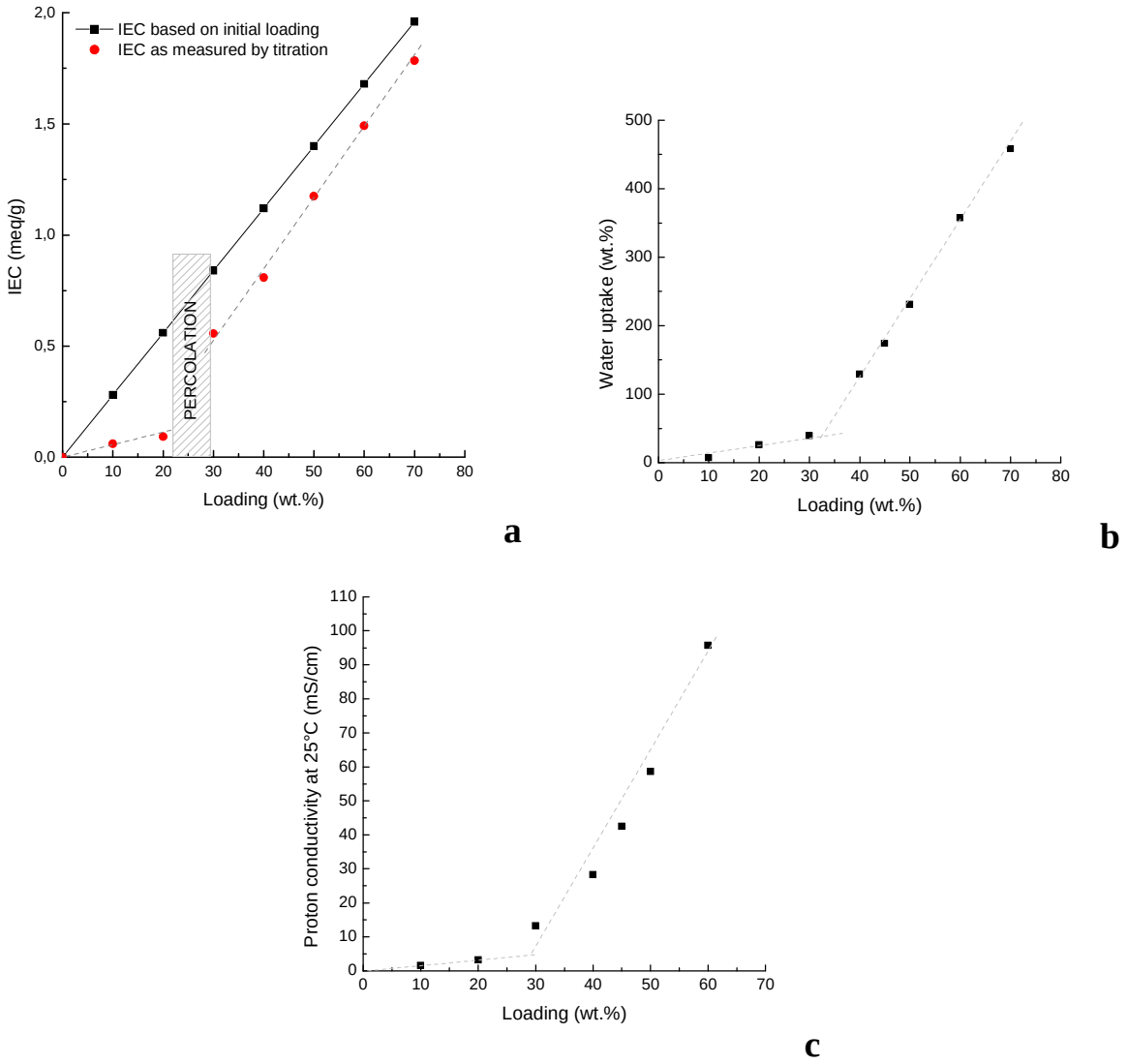

Figure S2. Influence of particles loading on membrane characteristics: variation of (a) theoretical and experimental Ionic Exchange Capacities, (b) water uptake, and (c) proton conductivity of hybrid membranes as a function of filler content at 25°C in liquid water.

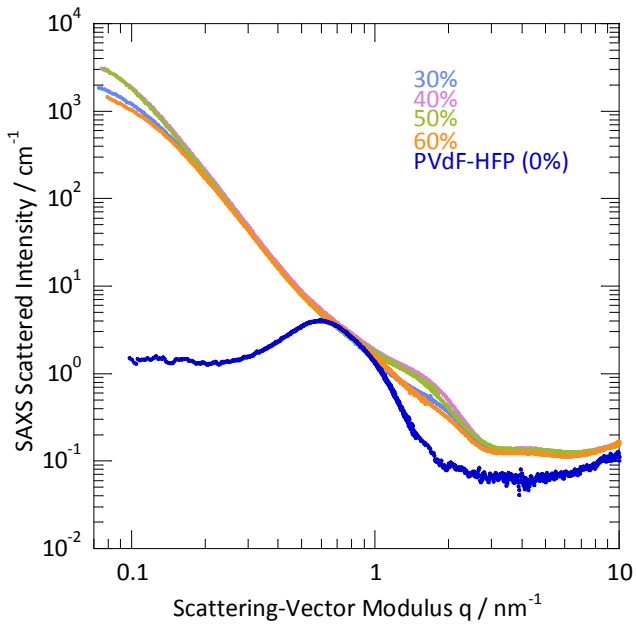

Figure. S3. SAXS absolute intensity as a function of the scattering-vector modulus for hydrated membranes at different loadings (wt.%) neutralized by Cs^+.

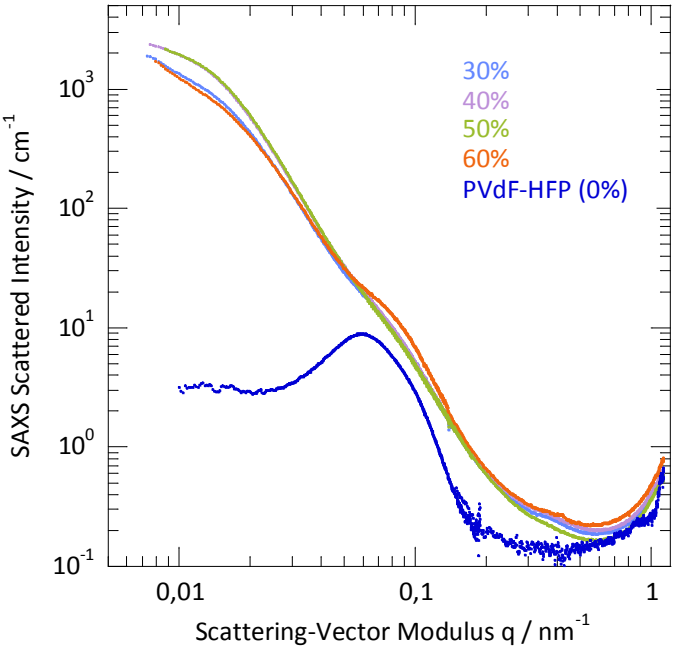

Figure. S4. SAXS absolute intensity as a function of the scattering-vector modulus for dried membranes at different loadings (wt.%) neutralized by Cs^+.

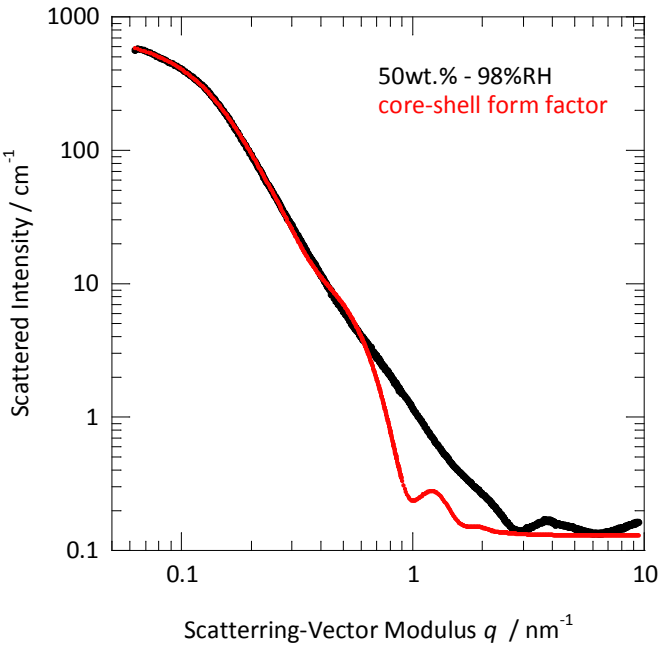

Figure S5. SAXS absolute intensity as a function of the scattering-vector modulus q for (i) a membrane with 50 wt.% of fillers surrounded by 98 %RH at room temperature, and (ii) a simulation of the form factor for core-shell spheres with shell thicknesses equal to 70 nm distributed according a Schulz distribution (σ=0.5) with a core radius equal to 60 nm.

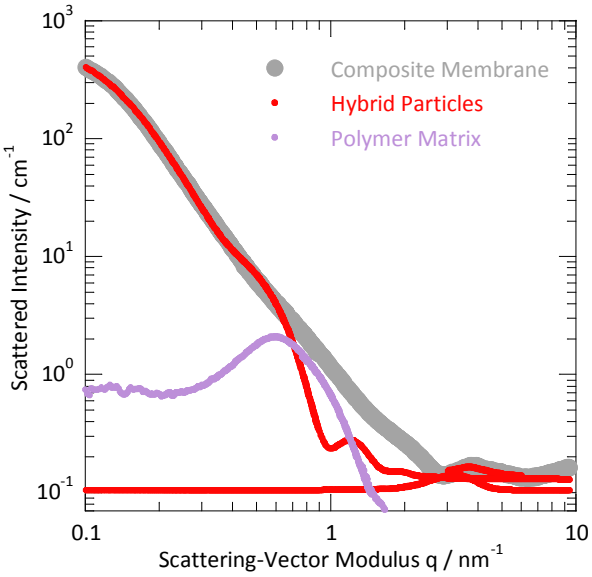

Figure S6. SAXS absolute intensity as a function of the scattering-vector modulus q for (i) a swelled membrane with 50 wt.% of fillers at room temperature, (ii) a simulation of the form factor due to the hybrid particles with core-shell spheres having shell thicknesses equal to 70 nm distributed according a Schulz distribution (σ=0.5) and a core radius equal to 60 nm as well as the contribution of the polyelectrolyte chains (Gaussian-shape distribution for the correlation lengths), and (iii) the experimental contribution of the polymer matrix.

M1: The **Debye-Anderson-Brumberger (DAB) model**, also named form factor of two-term **Debye-Bueche long distance correlation**, was used. This model is suitable to analyze the scattering from a randomly distributed, two-phase system based. The two-phase system is characterized by a single length scale, the correlation length, which is a measure of the average spacing between both regions. The model also assumes an exponential and isotropic decay of the electron-density correlation. The scattering density can be written as follows:

$$I(q) = \frac{A}{(1 + q^2 \cdot L_{DAB}{}^2)^2} + B$$

with A a scaling factor depending on the system, $\boldsymbol{L_{DAB}}$ **the correlation length** and B a background constant.

M2: The form factor of a hybrid particle and/or a compact aggregate of several ones, which is supposed to be spherical, is written as:

$$F(q)=(3\cdot f(q\cdot R))^2 \quad \text{with} \quad f(x)=\frac{\sin(x) - x\cdot\cos(x)}{x^3}$$

***R* is the radius of a particle or of compact spherical-like particles of a finite number of particles**. The studied polydisperse system is characterized by a continuous distribution of macroion's size and charges. An alternative method to model polydispersity in size and charges is to fit the data to an analytic function for the size distribution. A commonly used model for the macroion's size and charge distribution is the Schulz distribution function[4,5]. For the mean sphere radius with the sphere model, the Schultz distribution (h function) was used:

$$h(r)=\frac{(t+1)^{t+1}}{R}\left(\frac{r}{R}\right)^t \exp\left(-(t+1)\frac{r}{R}\right)\frac{1}{\Gamma(t+1)}$$

R is the mean sphere radius and t is a parameter related to the width of the distribution. In particular, one has a polydispersity index $p=\sigma/R$ where σ is the root-mean-square deviation from the mean size, given by $p=1/(1+t)^{1/2}$. This method was then used to extract the mean radius and polydispersity in terms of the normalized standard deviation. The form factor with polydispersity is then calculated by integration:

$$F(q)=\int h(r,R,\sigma)\cdot F(q,r)\cdot dr$$

M3: To accurately determinate the **crystallinity index (w_{cr})**, a "disorder" function would be taken into account.[6] This function permits to take into consideration the intensity decrease originating from variations of the atoms from their ideal positions. In a first approximation,[7] the crystallinity index can be defined with the following ratio of the integrated crystalline scattering to the total scattering:

$$w_{cr} = \frac{\int_0^\infty s^2 \cdot I_c \cdot ds}{\int_0^\infty s^2 \cdot I \cdot ds}$$

in which s is the reciprocal space vector, I_c the coherent intensity of the crystalline phase, and I the total coherent scattering. The computerization[8] and the improvement provided by Polizzi et alii[9] permit to estimate the error, in the present case, by using this approximation. Considering that (i) the amorphous and crystalline contributions are in the same angular range, and the third peak has a very low contribution with regard to the other ones, (ii) this

range is sufficiently weak to use this approach, the more accurate methods[9] show that the precision of the determination is, however, ±10%. Thus in the present case of an estimation of the crystallinity index, to take in consideration the imperfection factor is not necessary. This approximation is also valid insofar as the material in both the amorphous and the crystalline phases are the same ones.[7,10] The different hypotheses are expressed through the use of the following relation:

$$w_{cr} = \frac{\int_{q_0}^{q_1} q^2 \cdot I_c \cdot dq}{\int_{q_0}^{q_1} q^2 \cdot I \cdot dq}$$

in which q is the magnitude of the scattering vector ($q = (4\pi/\lambda)\cdot\sin\theta$), $2\theta_0 = 5°$ and $2\theta_1 = 40°$. In these ratios, the intensity curves of the membranes are weighted by q^2, which accounts for the Lorentz correction of the intensity curve,[11] especially in this case with all the contributions in the same range of angles and at pretty low angles.

M4: According to the **Debye-Scherrer equation**, the broadening due to small crystallite size may be expressed as:

$$L = \frac{k \cdot \lambda}{FWHM \cdot \cos\theta}$$

where L is the average crystallite size, FWHM the Full Width at Half Maximum, θ the Bragg's angle, k a constant whose value depends on particle shape and usually taken as 1.0, and λ the wavelength of incident X-ray beam.

(1) Niepceron, F.; Lafitte, B.; Galiano, H.; Bigarre, J.; Nicol, E.; Tassin, J. F. *J Membrane Sci* **2009**, *338*, 100.
(2) von Werne, T.; Patten, T. E. *J. Am. Chem. Soc.* **1999**, *121*, 7409.
(3) Xu, F. J.; Kang, E. T.; Neoh, K. G. *Macromolecules* **2005**, *38*, 1573.
(4) Zimm, B. H. *J. Chem. Phys.* **1948**, *16*, 1099.
(5) Wagner, N. J.; Krause, R.; Rennie, A. R.; Daguanno, B.; Goodwin, J. *J. Chem. Phys.* **1991**, *95*, 494.
(6) Ruland, W. *Acta Crystallogr.* **1961**, *14*, 1180.
(7) Alexander, L. E. *X-ray diffraction methods in polymer science*; Wiley-Interscience ed.; Wiley-Interscience: New York, 1969.
(8) Vonk, C. G. *J. Appl. Crystallogr.* **1973**, *6*, 148.
(9) Polizzi, S.; Fagherazzi, G.; Benedetti, A.; Battagliarin, M. *J. Appl. Crystallogr.* **1990**, *23*, 359.
(10) Abbrent, S.; Plestil, J.; Hlavata, D.; Lindgren, J.; Tegenfeldt, J.; Wendsjo, A. *Polymer* **2001**, *42*, 1407.
(11) Balta-Calleja, F.; Vonk, C. G. *X-ray Scattering of Synthetic Polymers*; Elsevier: Amsterdam, 1989.